Research Article

Possible zero sound in layered perovskites with ferromagnetic *s-d* exchange interaction

Todor M. Mishonov[1] · Nedelcho I. Zahariev[1] · Hassan Chamati[1] · Albert M. Varonov[1]

Received: 22 November 2021 / Accepted: 30 June 2022
Published online: 19 July 2022

Abstract
We analyze the conditions for observation of zero sound in layered perovskites with transition metal ion on chalcogenide oxidizer. We conclude that propagation of zero sound is possible only for a ferromagnetic sign of the *s-d* interaction. If the *s-d* exchange integral J_{sd} has antiferromagnetic sign, as it is perhaps in the case for layered cuprates, zero sound is a thermally activated dissipation mode, which generates only "hot spots" in the Angle Resolved Photoemission Spectroscopy (ARPES) data along the Fermi contour. We predict that zero sound will be observable for transition metal perovskites with 4*s* and 3*d* levels close to the *p*-level of the chalcogenide. The simultaneous lack of superconductivity, the appearance of hot spots in ARPES data, and the proximity of the three named levels, represents the significant hint for the choice of material to be investigated.

Article highlights

- Propagation of zero sound in layered transition metal perovskites is predicted in framework of s-d exchange interaction with ferromagnetic sign.
- It is revealed that strong exchange interaction is created by strong s-p-d hybridization between the transition ion and oxidant.
- The propagation of zero sound is possible only close to cold spots directions of the normal charge carriers along the Fermi contour.

Keywords Zero sound · *s-d* Exchange interaction · Hot spots · Cold spots · High-Tc superconductivity · Transverse sound modes

1 Introduction

The theoretical prediction of zero sound by Landau [1, 2] and subsequent experimental observations [3, 4] in ^{3}He was a powerful evidence of the applicability of Landau picture of Fermi quasi-particles excitations and their self-consistent motion to (strongly correlated) Fermi liquids. The zero Fermi sound in metals, more precisely zero spin sound, was observed in Cr metal [5, 6]. These experiments stimulated studies in the framework of the Hubbard model. Fuseya *et al.* [7] reached the important, to our further analysis, conclusion that Landau parameter, i.e. the averaged on the Fermi surface Fermi liquid interaction kernel $f(\mathbf{p}, \mathbf{q})$, can change its sign close

✉ Todor M. Mishonov, mishonov@bgphysics.eu; Nedelcho I. Zahariev, zahariev@issp.bas.bg; Hassan Chamati, chamati@issp.bas.bg; Albert M. Varonov, varonov@issp.bas.bg | [1]Georgi Nadjakov Institute of Solid State Physics, Bulgarian Academy of Sciences, 72 Tzarigradsko Chaussée, BG-1784 Sofia, Bulgaria.

to half filling of the conduction band. Later on Tsuruta [8] used two dimensional t-t' Hubbard model to study zero spin sound in antiferromagnetic metals. Here, we consider that this approach can be useful to study zero sound propagation and its importance from a materials science perspective. The purpose of the present paper is to explore the possibility of zero sound propagation in a layered perovskite with the structure of high-T_c having a CuO_2 conduction plane.

Postulating the interaction kernel $f(\mathbf{p},\mathbf{q})$ [9, Eq. (2.1)] between electrons with different momenta $\mathbf{p}$ and $\mathbf{q}$, we can explain different electronic phenomena in superconductivity and magnetism. The Fermi liquid approach provides results for the magnetic susceptibility, heat capacity, and effective masses. For illustration, in many cases the interaction is modeled by a separable kernel $f(\mathbf{p},\mathbf{q}) \propto \chi(\mathbf{p})\chi(\mathbf{q})$ and for our Hamiltonian separability holds.

The s-d exchange lies in the origin of the magnetic properties of transition metal compounds. Its most usual version was proposed by Schubin and Wonsovsky [10], Zener [11–13] and Kondo [14]. The purpose of the present study is to analyze whether the s-d exchange can lead to propagation of zero sound in transition metal compounds.

We anticipate here, that an anti-ferromagnetic sign of the s-d coupling J_{sd} leads to a singlet superconductivity while a ferromagnetic sign of J_{sd} is able to explain the repulsion necessary for the propagation of zero sound. We wish to emphasize that zero sound has not yet been observed in normal metals [15]. This may be traced back to the fact that the s-d exchange interaction was not used as a guide for the choice of appropriate materials.

In the next section we introduce the notions and notations developed to explain the electronic properties of the CuO_2 plane and its superconductivity, and analyze how a similar Hamiltonian would be used to predict zero sound in layered cuprates. Finally, we conclude that layered transition metal compounds may serve as the best candidates to search for zero sound in normal metals.

2 The s-d LCAO Hamiltonian for the CuO_2 plane in momentum p-representation

The Hamiltonian in the $\mathbf{r}$-representation is given in Ref. [16, Eq. (1.2)], here we start with the Hamiltonian in the $\mathbf{p}$-representation

$$\hat{H}' = \sum_{\mathbf{p},\,\alpha} \hat{\Psi}^{\dagger}_{\mathbf{p}} \left(H_{\mathrm{LCAO}} - \mu \mathbb{1}\right) \hat{\Psi}_{\mathbf{p}} - \frac{J_{sd}}{\mathcal{N}} \sum_{\substack{\mathbf{p}'+\mathbf{q}'=\mathbf{p}+\mathbf{q} \\ \alpha,\,\beta}} \hat{S}^{\dagger}_{\mathbf{q}',\beta} \hat{D}^{\dagger}_{\mathbf{p}',\alpha} \hat{S}_{\mathbf{p},\alpha} \hat{D}_{\mathbf{q},\beta}, \tag{1}$$

where

$$H_{\mathrm{LCAO}} \equiv \begin{pmatrix} \epsilon_d & 0 & t_{pd} s_x & -t_{pd} s_y \\ 0 & \epsilon_s & t_{sp} s_x & t_{sp} s_y \\ t_{pd} s_x & t_{sp} s_x & \epsilon_{\mathrm{p}} & -t_{pp} s_x s_y \\ -t_{pd} s_y & t_{sp} s_y & -t_{pp} s_x s_y & \epsilon_{\mathrm{p}} \end{pmatrix},$$

$$s_x \equiv 2\sin(p_x/2), \qquad s_y \equiv 2\sin(p_y/2),$$

$$\hat{\Psi}^{\dagger}_{\mathbf{p}} \equiv \left(\hat{D}^{\dagger}_{\mathbf{p},\alpha}\ \hat{S}^{\dagger}_{\mathbf{p},\alpha}\ \hat{X}^{\dagger}_{\mathbf{p},\alpha}\ \hat{Y}^{\dagger}_{\mathbf{p},\alpha}\right),$$

and the summation is actually an integration in the momentum space and $\mathcal{N} \gg 1$ is the total number of elementary cells for which we assume periodic boundary conditions

$$\frac{1}{\mathcal{N}} \sum_{\mathbf{p}} \cdots \equiv \iint\limits_{\{p_x,p_y\}\in(0,2\pi)} \frac{\mathrm{d}p_x \mathrm{d}p_y}{(2\pi)^2}$$

where the momentum variables are dimensionless phases $p_x, p_y, q_x, q_y \in (0, 2\pi)$; the dimensional momentum is $\mathbf{P} = (\hbar/a_0)\,\mathbf{p}$. In this LCAO Hamiltonian ϵ_s, ϵ_d and ϵ_p are the single site energies of an electron in Cu4s, Cu3$d_{x^2-y^2}$ and O2p states, t_{sp}, t_{pd} and t_{pd} are hopping amplitudes between neighboring orbitals. The s-d interaction is parameterized by the exchange integral J_{sd} which we consider as a

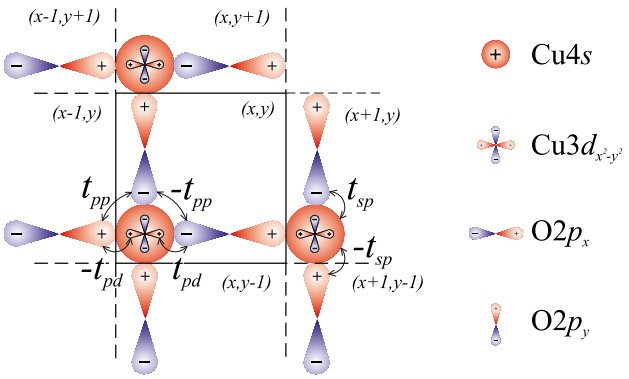

Fig. 1 Single electron processes in the conducting CuO_2 plane of layered cuprates after Ref. [16, Fig. 1.1]. LCAO is the basis of the chemical intuition. We have Hilbert space spanned over Cu4s, Cu3$d_{x^2-y^2}$, O2p_x, and O2p_y states. The LCAO Hamiltonian is parameterized by transfer integrals t_{pd}, t_{sp}, and t_{pp} and single site energies $\epsilon_d, \epsilon_s, \epsilon_p$

perturbation. Schematically, the atomic wave functions are depicted in Fig. 1. The chemical potential is denoted by μ and for the operator of the number of electrons we have the standard expression

$$\hat{N} = -\partial_\mu \hat{H}' = \sum_{\mathbf{p},\alpha} (\hat{D}^\dagger_{\mathbf{p},\alpha}\hat{D}_{\mathbf{p},\alpha} + \hat{S}^\dagger_{\mathbf{p},\alpha}\hat{S}_{\mathbf{p},\alpha} + \hat{X}^\dagger_{\mathbf{p},\alpha}\hat{X}_{\mathbf{p},\alpha} + \hat{Y}^\dagger_{\mathbf{p},\alpha}\hat{Y}_{\mathbf{p},\alpha}),$$

which we treat self-consistently.

2.1 Conduction band reduction

In order to derive the effective Hamiltonian describing the zero sound, we perform successive conduction band reductions. The first one is the number of particles. For notions and notations we follow the description of the electronic properties of the CuO_2 plane. In the hole doped phase of the CuO_2 plane we have 2 completely filled oxygen bands O2p and one partially filled Cu3$d_{x^2-y^2}$band, f is the relative number of holes in the Brillouin zone, i.e., the hole filling factor defined as the ratio of the area of the hole pocket around the (π, π) point and the area of the Brillouin zone is $(2\pi)^2$. For the averaged number of electrons we have

$$\frac{\langle \hat{N} \rangle}{\mathcal{N}} = 2 \times 2 + 2(1 - f). \tag{2}$$

For $f = \frac{1}{2}$ we have a pattern insulator, while for optimal doping we have

$$f_{\text{opt}} = \frac{1}{2} + 0.08. \tag{3}$$

The single electron component of the Hamiltonian is diagonalized in the $\mathbf{p}$-representation and we have to perform the summation over all four bands $b = 1, 2, 3, 4$

$$\hat{H}'^{(0)} = \sum_{\mathrm{b},\mathbf{p},\alpha} (\epsilon_{\mathrm{b},\mathbf{p}} - \mu)\hat{c}^\dagger_{\mathrm{b},\mathbf{p},\alpha}\hat{c}_{\mathrm{b},\mathbf{p},\alpha} \to \sum_{\mathbf{p},\alpha} (\epsilon_{\mathbf{p}} - \mu)\,\hat{c}^\dagger_{\mathbf{p},\alpha}\hat{c}_{\mathbf{p},\alpha}. \tag{4}$$

The spectrum $\mathbf{p}$ in the LCAO approximation is determined by the secular equation

$$\det[H_{\text{LCAO}} - \epsilon_{\mathbf{p}}\mathbb{1}] = \mathcal{A}xy + \mathcal{B}(x + y) + \mathcal{C} = 0,$$

where the variables

$$x = \sin^2\left(\frac{p_x}{2}\right), \qquad y = \sin^2\left(\frac{p_y}{2}\right),$$

are functions only of the momentum $\mathbf{p}$, and

$$\mathcal{A} = 32\left(t_{sp}^2 - \frac{1}{2}\varepsilon_s t_{pp}\right)^2 (2t_{pd}^2 + t_{pp}\varepsilon_d),$$
$$\mathcal{B} = -4\varepsilon_{\mathrm{p}}(t_{sp}^2\varepsilon_d + t_{pd}^2\varepsilon_s),$$
$$\mathcal{C} = \varepsilon_d\varepsilon_s\varepsilon_{\mathrm{p}}^2,$$

are polynomials of the energy ϵ. This analytical representation of the energy dispersion $\epsilon_{\mathbf{p}}$ allows to express explicitly its derivatives

$$\mathbf{v}_{\mathbf{p}} = \frac{\partial \epsilon_{\mathbf{p}}}{\partial \mathbf{p}}, \quad \mathbf{V}_{\mathbf{p}} = \frac{a_0}{\hbar}\mathbf{v}_{\mathbf{p}} = \frac{\mathrm{d}\mathbf{r}}{\mathrm{d}t}, \quad \mathbf{P} = \frac{\hbar}{a_0}\mathbf{p}, \tag{5}$$

where $\mathbf{P}$ is dimensional momentum and $V_{\mathbf{p}}$ is the velocity in the usual units length per time.

In order to study the low frequency electronic processes, we restrict the Hamiltonian summation only to the conduction band $b = 3$ and the index will be dropped; $b = 1$ and $b = 2$ denote completely filled oxygen bands, while $b = 4$ is the index for the completely empty Cu4s band. Performing this first reduction, the interaction s-d-exchange Hamiltonian reads

$$\hat{H}_{sd} = -\frac{J_{sd}}{\mathcal{N}} \sum_{\substack{\mathbf{p}'+\mathbf{q}'=\mathbf{p}+\mathbf{q} \\ \alpha,\beta}} S_{\mathbf{q}'} D_{\mathbf{p}'} \hat{c}^\dagger_{\mathbf{q}'\beta}\hat{c}^\dagger_{\mathbf{p}'\alpha}\hat{c}_{\mathbf{p}\alpha}\hat{c}_{\mathbf{q}\beta} S_{\mathbf{p}} D_{\mathbf{q}}, \tag{6}$$

where the real amplitudes

$$\begin{pmatrix} \tilde{D}_{\mathbf{p}} \\ \tilde{S}_{\mathbf{p}} \\ \tilde{X}_{\mathbf{p}} \\ \tilde{Y}_{\mathbf{p}} \end{pmatrix} = \begin{pmatrix} -\varepsilon_s\varepsilon_{\mathrm{p}}^2 + 4\varepsilon_p t_{sp}^2(x + y) - 32 t_{pp}\tau_{sp}^2 xy \\ -4\varepsilon_{\mathrm{p}} t_{sp} t_{pd}(x - y) \\ -(\varepsilon_s\varepsilon_{\mathrm{p}} - 8\tau_{sp}y)t_{pd}s_x \\ (\varepsilon_s\varepsilon_{\mathrm{p}} - 8\tau_{sp}x)t_{pd}s_y \end{pmatrix}$$

describe the amplitude of a band electron to be projected on Cu4s, Cu3$d_{x^2-y^2}$, O2p_x and O2p_y. For brevity we introduce the notations $\varepsilon_s = \epsilon - \epsilon_s, \varepsilon_d = \epsilon - \epsilon_d, \varepsilon_{\mathrm{p}} = \epsilon - \epsilon_{\mathrm{p}}$. The amplitudes have to be normalized to

$$C_\Psi = \frac{1}{\sqrt{D_{\mathbf{p}}^2 + S_{\mathbf{p}}^2 + X_{\mathbf{p}}^2 + Y_{\mathbf{p}}^2}},$$

and finally $S_{\mathbf{p}} = C_\Psi \tilde{S}_{\mathbf{p}}$, $D_{\mathbf{p}} = C_\Psi \tilde{D}_{\mathbf{p}}$. For convenience we introduce the notation describing the s-d hybridization amplitude $\chi_{\mathbf{p}} \equiv S_{\mathbf{p}} D_{\mathbf{p}}$ of the band electron. In the next subsection we juxtapose different further reductions of the exchange Hamiltonian treated in a self-consistent way.

2.2 BCS versus Fermi liquid reduction

Our first step is to perform BCS reduction of the exchange Hamiltonian Eq. (6). In the sum we have to take

into account only the annihilation and creation operators with opposite momenta and spins

$$\mathbf{q}' = -\mathbf{p}', \qquad \mathbf{q} = -\mathbf{p}, \qquad \beta = \overline{\alpha}. \tag{7}$$

In averaging of this BCS reduced Hamiltonian we apply the self-consistent approximation

$$\begin{aligned}\langle \hat{c}^{\dagger}_{\mathbf{q}'\beta}\hat{c}^{\dagger}_{\mathbf{p}'\alpha}\hat{c}_{\mathbf{p}\alpha}\hat{c}_{\mathbf{q}\beta}\rangle &\to \delta_{\mathbf{q}'+\mathbf{p}',0}\,\delta_{\mathbf{q}+\mathbf{p},0}\,\langle \hat{c}^{\dagger}_{\mathbf{q}'\beta}\hat{c}^{\dagger}_{\mathbf{p}'\alpha}\hat{c}_{\mathbf{p}\alpha}\hat{c}_{\mathbf{q}\beta}\rangle \\ &\approx \delta_{\mathbf{q}'+\mathbf{p}',0}\,\delta_{\mathbf{q}+\mathbf{p},0}\,\langle \hat{c}^{\dagger}_{\mathbf{q}'\beta}\hat{c}^{\dagger}_{\mathbf{p}'\alpha}\rangle\langle \hat{c}_{\mathbf{p}\alpha}\hat{c}_{\mathbf{q}\beta}\rangle \\ &= \langle \hat{c}^{\dagger}_{-\mathbf{p}'\overline{\alpha}}\hat{c}^{\dagger}_{\mathbf{p}'\alpha}\rangle\langle \hat{c}_{\mathbf{p}\alpha}\hat{c}_{-\mathbf{p}\overline{\alpha}}\rangle \\ &= \langle \hat{B}_{\mathbf{p}'}\rangle\langle \hat{B}_{\mathbf{p}}\rangle,\end{aligned}$$

where

$$\begin{aligned}\hat{B}_{\mathbf{p}} &\equiv \hat{c}_{-\mathbf{p},-}\hat{c}_{\mathbf{p}+} \\ &= u_{\mathbf{p}}v_{\mathbf{p}}(1-\hat{b}^{\dagger}_{-\mathbf{p},-}\hat{b}_{-\mathbf{p}-}-\hat{b}^{\dagger}_{\mathbf{p},+}\hat{b}_{\mathbf{p}+})+\dots\ .\end{aligned}$$

Colors (on-line) describe factorization of means in the effective Hamiltonian. The self-consistent approximation is reduced to substitution of averaged product of four operators to the product of averaged two operators. In order to emphasize the basis of the BCS approximation we use different colors. Those colors can be traced back to the conduction band reduced exchange Hamiltonian Eq. (6). We use standard notations for Bogolyubov *u-v* rotation and the new $\hat{B}$ operators with average expressed in terms of new Fermion number operators $\hat{n}_{\mathbf{p},\alpha} = \hat{b}^{\dagger}_{\mathbf{p}\alpha}\hat{b}_{\mathbf{p}\alpha}$. In this way the average exchange Hamiltonian is incorporated in the standard BCS scheme

$$\langle \hat{H}^{(\mathrm{BCS})}_{sd}\rangle = \frac{1}{\mathcal{N}}\sum_{\mathbf{p}',\mathbf{p}}\langle \hat{B}_{\mathbf{p}'}\rangle f(\mathbf{p}',\mathbf{p})\langle \hat{B}_{\mathbf{p}}\rangle, \tag{8}$$

where the kernel

$$f(\mathbf{p}',\mathbf{p}) = -2J_{sd}\chi_{\mathbf{p}'}\chi_{\mathbf{p}}.$$

is separable due to the fact that the exchange interaction is localized on a single ion in the elementary cell of the crystal.

Now we address the Fermi liquid reduction of the same exchange Hamiltonian Eq. (6) which we rewrite

$$\hat{H}_{sd} = -\frac{J_{sd}}{\mathcal{N}}\sum_{\substack{\mathbf{p}'+\mathbf{q}'=\mathbf{p}+\mathbf{q}\\ \alpha,\beta}} S_{\mathbf{q}'}D_{\mathbf{p}'}\hat{c}^{\dagger}_{\mathbf{q}'\beta}\hat{c}^{\dagger}_{\mathbf{p}'\alpha}\hat{c}_{\mathbf{p}\alpha}\hat{c}_{\mathbf{q}\beta}S_{\mathbf{p}}D_{\mathbf{q}}.$$

In order to point out the difference between BCS and Fermi liquid reduction now the colors mark the operators which will be grouped in the next self-consistent approximation. In the Fermi-liquid (FL) reduced Hamiltonian we have to take into account only the terms with

$$\mathbf{p}' = \mathbf{p}, \qquad \mathbf{q}' = \mathbf{q}. \tag{9}$$

In FL reduction we have again to apply the self-consistent approximation for the relevant terms

$$\begin{aligned}\langle \hat{c}^{\dagger}_{\mathbf{q}'\beta}\hat{c}^{\dagger}_{\mathbf{p}'\alpha}\hat{c}_{\mathbf{p}\alpha}\hat{c}_{\mathbf{q}\beta}\rangle &\to \delta_{\mathbf{q}',\mathbf{q}}\,\delta_{\mathbf{p}',\mathbf{p}}\,\langle \hat{c}^{\dagger}_{\mathbf{p}'\alpha}\hat{c}_{\mathbf{p}\alpha}\hat{c}^{\dagger}_{\mathbf{q}'\beta}\hat{c}_{\mathbf{q}\beta}\rangle \\ &\approx \delta_{\mathbf{q}',\mathbf{q}}\,\delta_{\mathbf{p}',\mathbf{p}}\,\langle \hat{c}^{\dagger}_{\mathbf{p}'\alpha}\hat{c}_{\mathbf{p}\alpha}\rangle\langle \hat{c}^{\dagger}_{\mathbf{q}'\beta}\hat{c}_{\mathbf{q}\beta}\rangle \\ &= \langle \hat{c}^{\dagger}_{\mathbf{p}\alpha}\hat{c}_{\mathbf{p}\alpha}\rangle\langle \hat{c}^{\dagger}_{\mathbf{q}\beta}\hat{c}_{\mathbf{q}\beta}\rangle \\ &= \langle n_{\mathbf{p},\alpha}\rangle\langle n_{\mathbf{q},\beta}\rangle.\end{aligned}$$

Analogously to the BCS reduction, now for the FL reduction we obtain the averaged Hamiltonian

$$\langle \hat{H}^{(\mathrm{FL})}_{\mathrm{sd}}\rangle = \frac{1}{\mathcal{N}}\sum_{\mathbf{p},\mathbf{q},\,\alpha,\beta}\langle \hat{n}_{\mathbf{p},\alpha}\rangle f(\mathbf{p},\mathbf{q})\langle \hat{n}_{\mathbf{q},\beta}\rangle, \tag{10}$$

which is expressed by the same kernel

$$f(\mathbf{p},\mathbf{q}) = -2J_{sd}\chi_{\mathbf{p}}\chi_{\mathbf{q}},$$

applied between the average numbers of the Fermi particles

$$\hat{n}_{\mathbf{p},\alpha} = \hat{c}^{\dagger}_{\mathbf{p}\boldsymbol{\alpha}}\hat{c}_{\mathbf{p}\boldsymbol{\alpha}},$$

$$\langle \hat{n}_{\mathbf{p},\alpha}\hat{n}_{\mathbf{q},\beta}\rangle \approx \langle \hat{n}_{\mathbf{p},\alpha}\rangle\langle \hat{n}_{\mathbf{q},\beta}\rangle.$$

This coincidence of the kernels of BCS and FL approach is one of the central results of the present study. This coincidence can be explored for application in the study of other layered transition metal perovskites as well.

We wish to emphasize that for the interaction kernel we have analytical results at hand and for the *s-d* hybridization function, we have [16]

$$\begin{aligned}\chi_{\mathbf{p}} &= S_{\mathbf{p}}D_{\mathbf{p}} \\ &= 4\varepsilon_{\mathrm{p}}t_{sp}t_{pd}(x-y) \\ &\quad\times\left[\varepsilon_s\varepsilon^2_{\mathrm{p}} - 4\varepsilon_{\mathrm{p}}t^2_{sp}(x+y) + 32t_{pp}\tau^2_{sp}xy\right] \\ &\quad\times\Big\{\left[4\varepsilon_{\mathrm{p}}t_{sp}t_{pd}(x-y)\right]^2 \\ &\qquad + \left[\varepsilon_s\varepsilon^2_{\mathrm{p}} - 4\varepsilon_{\mathrm{p}}t^2_{sp}(x+y) + 32t_{pp}\tau^2_{sp}xy\right]^2 \\ &\qquad + 4x\left[(\varepsilon_s\varepsilon_{\mathrm{p}} - 8\tau^2_{sp}y)t_{pd}\right]^2 \\ &\qquad + 4y\left[(\varepsilon_s\varepsilon_{\mathrm{p}} - 8\tau^2_{sp}x)t_{pd}\right]^2\Big\}^{-1}.\end{aligned} \tag{11}$$

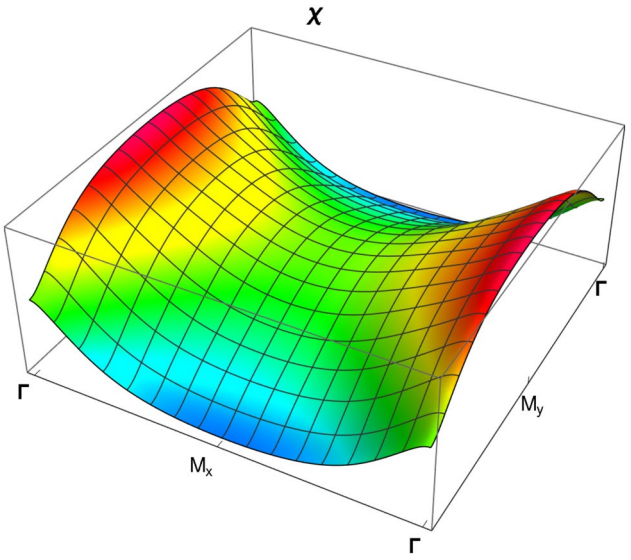

Fig. 2 The hybridization function $\chi_{\mathbf{p}} = S_p D_p$ representing the amplitude electron from conduction Cu3$d_{x^2-y^2}$ band being simultaneously a Cu4*s* electron. This is the main ingredient of the matrix elements of the *s-d* exchange interaction

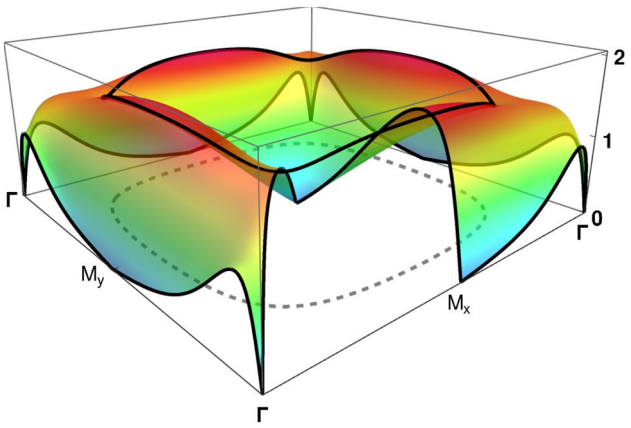

Fig. 3 Velocity $v_{\mathbf{p}}$ of the conduction band as a function of quasi-momentum p_x, $p_y \in (0, 2\pi)$ with dimension energy given in eV. The variable $V = (a_0/\hbar)v$ has dimension m/s. In the special points $\Gamma = (0, 0)$, $\mathrm{M} = (\pi, 0)$, $\mathrm{X} = (\pi, \pi)$ the band velocity $\mathbf{V} = \partial\epsilon_{\mathbf{P}}/\partial\mathbf{P}$ is zero; $\mathbf{P} = (\hbar/a_0)\mathbf{p}$

This hybridization function in the quasi-momentum representation is depicted in Fig. 2.

One can see that at fixed electron energy this saddle can be approximated by single sinusoidal approximation $\chi \propto \cos(2\theta)$ where $\theta = \arctan(p_y, p_x)$. Close to the (π, π)-point the single particle spectrum $\epsilon_{\mathbf{p}}$ has a parabolic form $\epsilon_{\mathbf{p}} \approx \epsilon_{\pi,\pi} - p^2/2\tilde{m}_{\mathrm{eff}}$ and qualitatively this approximation can be extended to the Fermi contour of the optimally doped cuprates.

The band velocity $\mathbf{v} = \partial_{\mathbf{p}}\epsilon_{\mathbf{p}}$ calculated from the real LCAO Hamiltonian is drawn in Fig. 3.

Here we can see that the circular Fermi contour is only a rough initial approximation.

The averaged BCS Hamiltonian has to be minimized with respect to $u_{\mathbf{p}}$ and then the BCS spectrum

$$E_{\mathbf{p}} = \frac{\partial\langle\hat{H}^{(\mathrm{BCS})}\rangle}{\partial\langle n_{\mathbf{p},\alpha}\rangle} = \sqrt{(\epsilon_{\mathbf{p}} - \mu)^2 + \Delta_{\mathbf{p}}^2}. \tag{12}$$

In the next Section we analyze the possible propagation of zero sound in layered perovskites using the single particle spectrum obtained from the FL reduced Hamiltonian Eq. (10).

3 Zero sound dispersion

For a concise introduction to the Fermi liquid approach we recommend the well-known monographs by Nozieres [17], Abrikosov [15], Abrikosov, Gor'kov and Dzyaloshinski [18], Lifshitz and Pitaevskii [9] and [19, Sec. 76].

Introducing for brevity $n_{\mathbf{p},\alpha} \equiv \langle\hat{n}_{\mathbf{p},\alpha}\rangle$, the averaged FL Hamiltonian Eq. (10) reads

$$\begin{aligned} H_{\mathrm{FL}} &\equiv \langle\hat{H}^{(\mathrm{FL})}\rangle \\ &= \sum_{\mathbf{p},\alpha} \epsilon_{\mathrm{p}} n_{\mathrm{p},\alpha} + \frac{1}{\mathcal{N}} \sum_{\mathbf{p},\mathbf{q},\alpha,\beta} n_{\mathbf{p},\alpha} f(\mathbf{p},\mathbf{q}) n_{\mathbf{q},\beta}. \end{aligned} \tag{13}$$

Notice that the spin indices may be omitted if we consider spin non-polarized phenomena, such that $n_{\mathbf{q},+} = n_{\mathbf{q},-}$. Introducing $n_{\mathbf{q}} \equiv n_{\mathbf{q},+} + n_{\mathbf{q},-} = 2n_{\mathbf{q},+} = 2n_{\mathbf{q},-}$ for the FL energy spectrum we get

$$\begin{aligned} \varepsilon(\mathbf{p},\mathbf{r}) &= \frac{\partial H_{\mathrm{FL}}}{\partial\hat{n}_{\mathbf{p}}} \\ &= \epsilon_{\mathbf{p}} + \frac{1}{\mathcal{N}} \sum_{\mathbf{q}} f(\mathbf{p},\mathbf{q}) n_{\mathbf{q}}(\mathbf{r}) \\ &= \epsilon_{\mathbf{p}} + \frac{(-2J_{sd})}{\mathcal{N}} \chi_{\mathbf{p}} \sum_{\mathbf{q}} \chi_{\mathbf{q}} n_{\mathbf{q}}(\mathbf{r},t), \end{aligned} \tag{14}$$

where the space variable $\mathbf{r} \equiv a_0\mathbf{n}$ can be introduced only in the quasi-classical WKB approximation. The *s-d* hybridization function Eq. (11) determines both the gap anisotropy $\Delta_{\mathbf{p}}(T) = \Xi(T)\chi_{\mathbf{p}}$ and the FL interaction. A detailed analysis of the gap anisotropy and the hot/cold spot anisotropy of ARPES data described by the hybridization function $\chi_{\mathbf{p}}$ in Eq. (11) is presented in Ref. [20]. Now we consider the momentum distribution $n_{\mathbf{p}}(\mathbf{r},t)$ of the charge carriers as

dynamic variables. Assuming a local deformation of the Fermi contour in two dimensions

$$n_{\mathbf{p}}(\mathbf{r},t) = 2\,\theta(\epsilon_{_F} + \nu_{\mathbf{p}}(\mathbf{r},t) - \epsilon_{\mathbf{p}}),$$
$$n^{(0)}_{\mathbf{p},+} = n^{(0)}_{\mathbf{p},-} = \theta(\epsilon_{_F} - \epsilon_{\mathbf{p}}),$$
$$\delta n_{\mathbf{p}} = n_{\mathbf{p}}(\mathbf{r},t) - n^{(0)}_{\mathbf{p}}$$

and using the collisionless Boltzmann equation, we derive the integral equation for the deformation of the Fermi contour. In the linearized with respect to small ν equation we assume plane wave perturbations, i.e.,

$$\delta n_{\mathbf{p}}(\mathbf{r},t) \approx 2\,\delta(\epsilon_{_F} - \epsilon_{\mathbf{p}})\nu_{\mathbf{p}}\exp[\mathrm{i}(\mathbf{K}\cdot\mathbf{r} - \omega t)], \tag{15}$$

with wavevector $\mathbf{K} = \mathbf{k}/a_0$ and frequency ω.

The WKB energy $\varepsilon(\mathbf{p},\mathbf{r})$ from Eq. (14) is actually an effective Hamiltonian which gives the force acting on the electrons

$$\mathbf{F}_{\mathbf{p}}(\mathbf{r},t) = -\frac{\partial\varepsilon(\mathbf{p},\mathbf{r})}{\partial\mathbf{r}} = \frac{\mathrm{d}\mathbf{P}}{\mathrm{d}t} \tag{16}$$

and together with the substitution Eq. (15) of $n_{\mathbf{p}}(\mathbf{r},t)$ gives

$$\mathbf{F}_{\mathbf{p}}(\mathbf{r},t) = -\mathrm{i}\mathbf{K}\int_{\mathrm{BZ}} f(\mathbf{p},\mathbf{p}')\,\delta n_{\mathbf{p}'}\frac{\mathrm{d}p'_x\mathrm{d}p'_y}{(2\pi)^2}. \tag{17}$$

The substitution of the small deformation of the Fermi contour $\delta n_{\mathbf{p}}$ from Eqs. (14) and (15) in the collisionless Boltzmann equation

$$\frac{\mathrm{d}}{\mathrm{d}t}\,\delta n_{\mathbf{p}}(\mathbf{r},t) = \frac{\partial\delta n_{\mathbf{p}}}{\partial t} + \frac{\partial\delta n_{\mathbf{p}}}{\partial\mathbf{P}}\cdot\mathbf{F}_{\mathbf{p}} + \frac{\partial\delta n_{\mathbf{p}}}{\partial\mathbf{r}}\cdot\mathbf{V}_{\mathbf{p}} = 0 \tag{18}$$

after some algebra leads to the dispersion equation

$$\big(\omega - \mathbf{K}\cdot\mathbf{V}_F(\mathbf{p})\big)\nu_{\mathbf{p}} = \frac{\mathbf{K}\cdot\mathbf{V}_F(\mathbf{p})}{(2\pi)^2}\oint_{\mathrm{FC}} f(\mathbf{p},\mathbf{p}')\nu_{\mathbf{p}'}\frac{\mathrm{d}p'_l}{v_F(p'_l)}, \tag{19}$$

where

$$K_x = K\cos\beta, \quad K_y = K\sin\beta, \quad \mathbf{k} = a_0\mathbf{K}.$$

To proceed further we introduce the averaging on the Fermi contour

$$\langle F\rangle \equiv \frac{1}{\rho_{_F}}\oint_{\mathrm{FC}} F(\mathbf{p})\,\frac{\mathrm{d}p_l}{(2\pi)^2 v_F(\mathbf{p})},$$

where

$$\rho_{_F} \equiv \oint_{\mathrm{FC}} 1\,\frac{\mathrm{d}p_l}{(2\pi)^2 v_F(\mathbf{p})}$$

is the density of electronic states per elementary cell and spin. For the separable kernel of the *s-d* interaction the dispersion equation for the zero sound reads

$$\hbar\omega\langle\chi\nu\rangle - \mathbf{k}\cdot\langle\mathbf{v}\chi\nu\rangle = (-2J_{sd})\rho_{_F}\mathbf{k}\cdot\langle\mathbf{v}\chi^2\rangle\langle\chi\nu\rangle,$$

where the momentum argument of all those average values is omitted for brevity. In order to analyze qualitatively the solutions of this integral equation for $\nu(\mathbf{p})$ we approximate the Fermi contour with a circle $\epsilon_{\mathbf{p}} = \mathbf{P}^2/2m_{\mathrm{eff}}$ and assume that the separable kernel behaves as a single sinusoidal on the Fermi contour

$$V_{\mathbf{p},\mathbf{q}'} \approx I_{sd}\,\cos(2\theta)\cos(2\theta'), \tag{20}$$

where

$$I_{sd} \approx -2J_{sd}\left[\frac{t_{sp}t_{pd}}{(\epsilon_s - \epsilon_d)(\epsilon_d - \epsilon_{\mathrm{p}})}\right]^2,$$
$$p_x = p\cos\theta, \quad p_y = p\sin\theta,$$
$$q'_x = q'\cos\theta', \quad q'_y = q'\sin\theta',$$
$$\frac{p^2}{2\tilde{m}_{\mathrm{eff}}} = \frac{q^2}{2\tilde{m}_{\mathrm{eff}}} = \epsilon_{_F}.$$

It is worth mentioning that many authors just postulate such a separable kernel for the pairing interaction $\chi \propto \cos(2\theta)$, while we have derived it from the *s-d* microscopic Hamiltonian.

If we analyze the propagation of zero sound along the nodal lines of the hybridization function $\beta = \pi/4$ the electric current and charge density oscillations are zero. In the general case for significant charge density oscillations the zero sound is actually a plasmon.

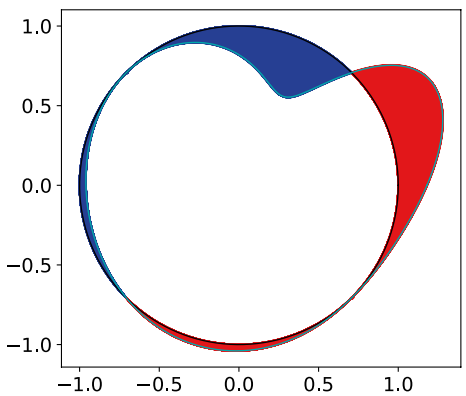

Fig. 4 Deformation of the Fermi contour in two dimensional momentum space $\mathbf{p}/\pi$ for zero sound propagating along "cold spots" [21] diagonal $\beta = \pi/4$ in layered perovskites. For this special case of propagation along the nodal lines of the separable kernel of interaction, the electric charge, spin and current oscillations are zero. Moreover, we have a shear deformation of the Fermi surface in momentum space

The deformation of the Fermi circle in this special case $\beta = \pi/4$ is depicted in Fig. 4.

For propagation of zero sound along other directions it is necessary to take into account the Coulomb repulsion and zero sound will behave partially as a plasmon in a layered structure. For a general review on plasmons in cuprate superconductors see Ref. [22].

4 Conclusion and discussion

We investigated the propagation of the zero sound in a class of layered transition metal perovskites involving a *s-d* interaction. We started and focused our attention on the CuO_2 plane that is a well-studied system. We were able to compare BCS and Fermi liquid reductions of the Hamiltonian and as a property of CuO_2 plane these two model Hamiltonian coincided. Moreover, we studied the influence of the sign of J_{sd} coupling. For anti-ferromagnetic sign we have tendency to superconductivity, while for ferromagnetic sign we expect zero sound to be observed.

Unfortunately at the moment, starting with a theoretical scheme, it is difficult to conclude in which layered compounds the zero sound will have the longest lasting propagation and what material is technologically suitable to produce a clean *ac*-surface. It is most likely that a thin layer geometry would provide a solution.

Owing to the research outlined throughout this paper we conclude: First of all, zero sound exists only when J_{sd} is negative and the *s-d* interaction has a ferromagnetic sign. However, the *s-d* exchange can create superconductivity only for antiferromagnetic sign (positive J_{sd}) of the exchange interaction. We arrive to the conclusion that in the normal phase of high-T_c cuprates propagation of zero sound is impossible. Zero sound for high-T_c cuprates is a dissipation mode, but thermal excitation of all those modes creates intensive scattering and Ohmic resistivity due to the exchange interaction and this strong angular dependence of the scattering rate is the cause of so called "hot spots" phenomenologically postulated for the interpretation of the experimental data [23]. Here we wish to add that thermal fluctuations of plasmons could also contribute to the hot spots along the Fermi contour [22].

Thermally agitated plasmons are related to electron density fluctuations which create electron scattering and ohmic resistivity due to exchange interaction. However, not for all doping levels the cuprates are superconducting and we do not exclude J_{sd} to change its sign for some compounds.

Our main motivation to write this paper is to attract the attention of experimentalists with appropriate samples at hand to probe the zero-sound propagation in the *ab*-plane of transition metal layered perovskites. If Angle Resolved Photoemission Spectroscopy (ARPES) data are available for these materials, hot spots along the Fermi contour or even smearing of this contour will be a significant hint for intensive *s-d* exchange which can lead to propagation of zero sound. In normal metals, the anisotropy of the electron-electron interaction is not strong enough to ensure zero sound propagation, but for layered perovskites such a phenomenon is most likely to occur. Another hint for intensive *s-d* exchange can come from band calculations, the hybridization is strongest if all those three levels: for transition ion 4*s* and 3*d* and *p*-states for the chalcogen are close to each other and we have almost a triple coincidence (full overlapping).

From the practical point of view, a possible route towards the excitation of the zero sound could be achieved by an intense perturbation from one side of a narrow strip, and detection on the opposite side of the sample. This, however is still a remote possibility.

Last but not least, already a half century ago different kinds of zero sound are extensively studied by theoretical means. This topic continues to attract a great deal of interest within the scientific community. Here we mention but a few papers that are somehow directly linked to our study. Recent considerations include the two-dimensional zero-sound [24] and shear [25] zero sound for *p*-type interaction [26], and we finally conclude that except for ^{3}He thin films and even two dimensional structures with large exchange interaction with ferromagnetic sign soon will become an interesting object for realization of the old idea of Landau [1, 2].

In this paper we have devised the theoretical framework for the possible emergence of zero sound in some layered perovskites involving ferromagnetic *s-d* exchange interaction. We will continue our effort to extend the investigation to other transition-metal compounds along with distinct geometries to put the test the plausibility of the present theory. From the experimental side we hope that the current technological progress would make it possible to synthesize appropriate compounds allowing for the propagation of zero sound.

5 Conclusion

The authors are thankful to Davide~Valentinis for the interest to the present study and pointing out for recently appeared related works on kinetic theories for the electrodynamic response of Fermi liquids and anisotropic metals [27–29].

Acknowledgments The authors AMV, TMM and NIZ are grateful to Cost Action CA16218 for the support in presenting the first results of the current research at the 7th International Conference on Superconducitvity and Magnetism in Bodrum, Turkey in 2021 and presenting the final version at the CA16218 meeting in Madrid, Spain in 2022.

Author Contributions All authors TMM, NIZ, HC and AMV contributed equally to this work.

Funding This work is supported by Grant No КП-06-H38/6 of the Bulgarian National Science Fund.

Data availability The data generated within this research is included in the paper.

Code availability Not applicable.

Declarations

Competing interests The authors have no relevant financial or non-financial interests to disclose.

Ethical approval Not applicable.

Consent to participate Not applicable.

Consent for publication Not applicable.

References

1. Landau LD (1956) The theory of a fermi liquid. Sov Phys JETP 3:920–925
2. Landau LD (1957) Oscillations in a fermi liquid. Sov Phys JETP 5:101–108
3. Keen BE, Matthews PW, Wilks J, Bleaney B (1965) The acoustic impedance of liquid helium-3. Proc R Soc A 284(1396):125–136. https://doi.org/10.1098/rspa.1965.0055
4. Abel WR, Anderson AC, Wheatley JC (1966) Propagation of zero sound in liquid He^3 at low temperatures. Phys Rev Lett 17:74–78. https://doi.org/10.1103/PhysRevLett.17.74
5. Fukuda T, Endoh Y, Yamada K, Takeda M, Itoh S, Arai M, Otomo T (1996) Dynamical magnetic structure of the spin density wave state in Cr. J Phys Soc Jpn 65(5):1418–1426. https://doi.org/10.1143/JPSJ.65.1418
6. Endoh Y, Fukuda T, Nakajima K, Kakurai K (1997) Polarized neutron studies for Cr excitations. J Phys Soc Jpn 66(6):1615–1617. https://doi.org/10.1143/JPSJ.66.1615
7. Fuseya Y, Maebashi H, Yotsuhashi S, Miyake K (2000) Anomalous fermi liquid effects in two-dimensional hubbard model near half-filling. J Phys Soc Jpn 69(7):2158–2163. https://doi.org/10.1143/JPSJ.69.2158
8. Tsuruta A, Hattori K, Ohta R, Miyake K (2010) Zero spin sound in antiferromagnetic metals: case of two-dimensional t-t' hubbard model. J Phys Soc Jpn 79(8):084710. https://doi.org/10.1143/JPSJ.79.084710
9. Lifshitz EM, Pitaevskii LP (1980) Statistical physics. Part 2. Landau-Lifshitz course of theoretical physics, vol 9. Pergamon, New York
10. Schubin S, Wonsowsky S (1934) On the electron theory of metals. Proc R Soc Lond Ser A 145(854):159–180. https://doi.org/10.1098/rspa.1934.0089
11. Zener C (1951) Interaction between the *d* shells in the transition metals. Phys Rev 81:440–444. https://doi.org/10.1103/PhysRev.81.440
12. Zener C (1951) Interaction between the *d*-shells in the transition metals. II. Ferromagnetic compounds of manganese with perovskite structure. Phys Rev 82:403–405. https://doi.org/10.1103/PhysRev.82.403
13. Zener C (1951) Interaction between the *d*-shells in the transition metals. III. Calculation of the Weiss Factors in Fe Co, and Ni. Phys Rev 83:299–301. https://doi.org/10.1103/PhysRev.83.299
14. Kondo J (1966) Anomalous scattering due to s-d interaction. J Appl Phys 37(3):1177–1180. https://doi.org/10.1063/1.1708385
15. Abrikosov AA (1988) Fundamentals of the theory of metals. North Holland, Amsterdam
16. Mishonov TM, Penev ES (2010) Theory of high temperature superconductivity. A conventional approach. World Scientific, New Jersey
17. Nozières P, Pines D (1966) The theory of quantum liquids, 1st edn. CRC Press, Boca Raton
18. Abrikosov AA, Gor'kov LP, Dzyaloshinskii IY (1963) Methods of quantum field theory in statistical physics. Prentice Hall, Englewood Cliffs
19. Lifshitz EM, Pitaevskii LP (1980) Physical kinetics. Landau-Lifshitz course of theoretical physics, vol 10. Pergamon, New York
20. Mishonov TM, Zahariev NI, Chamati H, Varonov AM (2021) Hot spots along the Fermi contour of high-T_c cuprates explained by *s-d* exchange interaction. SN Appl Sci. https://doi.org/10.1007/s42452-022-05106-9
21. Ioffe LB, Millis AJ (1998) Zone-diagonal-dominated transport in high-T_c cuprates. Phys Rev B 58(17):11631–11637. https://doi.org/10.1103/PhysRevB.58.11631
22. Greco A, Yamase H, Bejas M (2019) Origin of high-energy charge excitations observed by resonant inelastic x-ray scattering in cuprate superconductors. Commun Phys 2:3. https://doi.org/10.1038/s42005-018-0099-z
23. Hlubina R, Rice TM (1995) Resistivity as a function of temperature for models with hot spots on the Fermi surface. Phys Rev B 51:9253–9260. https://doi.org/10.1103/PhysRevB.51.9253
24. Khoo JY, Villadiego IS (2019) Shear sound of two-dimensional Fermi liquids. Phys Rev B 99(7):075434. https://doi.org/10.1103/PhysRevB.99.075434
25. Valentinis D, Zaanen J, van der Marel D (2021) Propagation of shear stress in strongly interacting metallic Fermi liquids enhances transmission of terahertz radiation. Sci Rep 11(1):1–13. https://doi.org/10.1038/s41598-021-86356-2
26. Ding S, Zhang S (2019) Fermi-liquid description of a single-component fermi gas with *p*-wave interactions. Phys Rev Lett 123:070404. https://doi.org/10.1103/PhysRevLett.123.070404

27. Valentinis D (2021) Optical signatures of shear collective modes in strongly interacting Fermi liquids. Phys Rev Res 3(2). https://doi.org/10.1103/PhysRevResearch.3.023076
28. Valentinis D, Baker G, Bonn DA, Schmalian J (2022) Kinetic theory of the non-local electrodynamic response in anisotropic metals: skin effect in 2D systems. arXiv. https://doi.org/10.48550/ARXIV.2204.13344. https://arxiv.org/abs/2204.13344
29. Baker G, Branch TW, Day J, Valentinis D, Oudah M, McGuinness P, Khim S, Surówka P, Moessner R, Schmalian J, Mackenzie AP, Bonn DA (2022) Non-local microwave electrodynamics in ultra-pure PdCoO2. arXiv. https://doi.org/10.48550/ARXIV.2204.14239. https://arxiv.org/abs/2204.14239